

1 **Supplementary Material**

2 **A Simple Strategy for Synthesis of *b*-Axis-Oriented MFI Zeolite Macro-Nanosheets**

3  
4 Wenshu Tai,<sup>1</sup> Weijiong Dai,<sup>1</sup> Guangjun Wu<sup>1,2\*</sup> and Landong Li<sup>1,2\*</sup>

5  
6 **EXPERIMENTAL SECTION**

7 **Chemicals and reagents:**

8 Tetraethylorthosilicate (TEOS, 99%, Aladdin), tetrapropylammonium hydroxide  
9 solution (TPAOH, 25 wt.%, InnoChem Chemical Reagents Company), sulfuric acid  
10 ( 95%~98% , Tianjin Chemical Reagent ), hydrochloric acid ( 36%~38%, Tianjin  
11 Chemical Reagent ), Acetic acid (C<sub>2</sub>H<sub>4</sub>O<sub>2</sub>, 99.5%, Shanghai Macklin Biochemical  
12 Technology Co., LTD ), Oxalic acid dehydrate ( H<sub>2</sub>C<sub>2</sub>O<sub>4</sub>·2H<sub>2</sub>O, 99.5%, Tianjin Guangfu  
13 Technology Development Co., LTD ), Lithium sulfate ( Li<sub>2</sub>SO<sub>4</sub>, 98.5%, Aladdin ),  
14 Sodium sulfate ( Na<sub>2</sub>SO<sub>4</sub>, 99%, Energy Chemical ), Potassium sulfate ( K<sub>2</sub>SO<sub>4</sub>, 99%,  
15 Aladdin ), Magnesium sulfate ( MgSO<sub>4</sub>, 99%, Beijing Shiji ), tetrabutyl titanate ( TBOT,  
16 TCI (SHANGHAI) Development Co., LTD ), Sodium aluminate (NaAlO<sub>2</sub>, 45% Al<sub>2</sub>O<sub>3</sub>,  
17 Tianjin Guangfu Fine Chemical Research Institute).

18 **Synthesis of MFI (Silicalite-1, S-1) ZMNs:**

19 To synthesize the S-1 ZMNs, the molar composition of 1.0 SiO<sub>2</sub>: x TPAOH: 25 H<sub>2</sub>O  
20 was used, where x = 0.1 ~ 0.3. A typical experiment involved mixing 18.7 g TEOS, 14 g  
21 H<sub>2</sub>O, and 10.85 g TPAOH with the molar composition of 1.0 SiO<sub>2</sub>: 0.15 TPAOH: 25 H<sub>2</sub>O  
22 at room temperature. The mixture was then aged at 90 °C for 12 h while stirring. Next,  
23 1.8 mol/L of H<sub>2</sub>SO<sub>4</sub> and 18 g H<sub>2</sub>O were added to the mixture to adjust the pH of the gel,  
24 which was then vigorously stirred at 90 °C for another 12 h. Finally, the gel was placed  
25 into a Teflon-lined steel autoclave and kept at static conditions at 90 ~ 180 °C for 3 days  
26 (unless stated otherwise). The resulting solid products were collected through filtration



© The Author(s) 2021. Open Access This article is licensed under a Creative Commons Attribution 4.0 International License (<https://creativecommons.org/licenses/by/4.0/>), which permits unrestricted use, sharing, adaptation, distribution and reproduction in any medium or format, for any purpose, even commercially, as long as you give appropriate credit to the original author(s) and the source, provide a link to the Creative Commons license, and indicate if changes were made.

27 or centrifugation, washed with deionized water, and dried overnight at 80 °C. Calcination  
28 was performed at 550 °C for 6 h in the air if needed.

### 29 **Synthesis of heteroatom-containing MFI ZMNs:**

30 MFI ZMNs containing heteroatoms have also been synthesized using 1.0 SiO<sub>2</sub>: 0.15  
31 TPAOH: 0.02 M: 25 H<sub>2</sub>O as the gel composition, where M is either Al<sub>2</sub>O<sub>3</sub> or TBOT.  
32 Specifically, 0.61 g of TBOT was combined with 18.7 g of TEOS, 10.85 g of TPAOH,  
33 and 14 g of H<sub>2</sub>O at room temperature. The detailed procedures are similar to those used  
34 for the synthesis of S-1 ZMNs, except that the crystallization temperature was maintained  
35 at 150 °C. In a similar manner, NaAlO<sub>2</sub> was introduced into the synthesis gel instead of  
36 TBOT, while keeping all the other procedures unchanged.

### 37 **Characterization:**

38 X-ray diffraction (XRD) patterns were recorded on a Rigaku Smart Lab 3kW  
39 diffractometer using Cu-K $\alpha$  radiation ( $\lambda = 0.1541$  nm) in the region of  $2\theta = 5^\circ \sim 50^\circ$ , and  
40 the degree of crystallinity was calculated by comparing the sum of the areas below the  
41 dominant peaks between  $2\theta = 22.5^\circ \sim 25^\circ$ .

42 Ar adsorption - desorption isotherms were obtained with a Quantachrome iQ-MP gas  
43 adsorption analyzer at -186 °C (87 K). The total surface area was calculated via the  
44 Brunauer-Emmett-Teller (BET) equation and the micropore volume was determined  
45 using the t-plot method.

46 Field-emission scanning electron microscope (FE-SEM) images were obtained on  
47 JSM-7800F.

48 High-resolution transmission electron microscopy (HR-TEM) images and the selected  
49 area electron diffraction (SAED) patterns were recorded on a JEOL JEM-2800 electron  
50 microscope.

51 Fourier transform infrared (FTIR) spectra were characterized by a Bruker Tensor 27  
52 spectrometer with 128 scans at a resolution of 2 cm<sup>-1</sup>, using KBr pellets.

53 <sup>29</sup>Si MAS NMR and <sup>27</sup>Al MAS NMR spectra were performed on Bruker Avance III  
54 WB 400 spectrometer at resonance frequency of 79.5 and 104.3 MHz. The <sup>29</sup>Si NMR  
55 spectra were recorded with a sample spinning rate of 5 kHz using a 7 mm MAS NMR  
56 probe.

57 Diffuse reflectance ultraviolet-visible (UV-Vis) spectra were recorded over the range  
58 of 200 to 800 nm with a blank sample as the reference, on a Perkin Elmer (Lambda 750)  
59 spectrophotometer.

### 60 Kinetic Study:

61 Kinetic study can be explored by plotting the crystallinity against the crystallization  
62 time, resulting in a crystallization curve. To investigate the kinetic behavior, the reaction  
63 was conducted using the optimum composition of 1.0 SiO<sub>2</sub>: 0.15 TPAOH: 25 H<sub>2</sub>O  
64 crystallized for various reaction times at 90, 100, 110 and 120 °C, respectively.

65 The Avrami-Erofeev equation (eq-1) was employed to describe the changes in MFI  
66 crystals over time during crystallization.<sup>[1]</sup>

$$67 \quad \alpha = 1 - e^{-k(t-t_0)^n} \quad (1)$$

68 where  $\alpha$  is the degree of crystallinity (0 to 1),  $t$  is the crystallization time,  $t_0$  is the  
69 induction time,  $k$  is the kinetic constant for crystalline growth in  $t^{-n}$  units,  $n$  is the  
70 Avrami's exponent, which is related with the crystallization mechanism.<sup>[2]</sup>

71 The values of  $n$  and  $k$  can be obtained using the following equation,<sup>[2]</sup> which is  
72 expressed by taking the double logarithm of eq-1.

$$73 \quad \ln[-\ln(1 - \alpha)] = n \ln(t - t_0) + \ln k \quad (2)$$

74 The growth rate of MFI crystals was calculated using the first derivative of eq-1.

$$75 \quad \frac{d\alpha}{dt} = kn(t - t_0)^{(n-1)} \cdot e^{-k(t-t_0)^n} \quad (3)$$

76 The inflection point of the crystallization stage, which corresponds to the steepest  
77 slope on the crystallization curve, was chosen as the crystallization rate ( $v_c$ ).<sup>[3]</sup> The  
78 inflection point existing in the crystallization stage was obtained by setting the second  
79 derivative of eq-1 to zero.

$$80 \quad \frac{d^2\alpha}{dt^2} = kn(n - 1)(t - t_0)^{(n-2)} \cdot e^{-k(t-t_0)^n} - k^2n^2(t - t_0)^{(2n-2)} \cdot e^{-k(t-t_0)^n} \quad (4)$$

81 The transition period ( $t_{tr}$ ) was determined by projecting the tangent line from the  
82 inflection point to the  $x$  axis within the crystallization curve.<sup>[2]</sup>

83 The values of activation energy ( $E$ ) and preexponential factor ( $\ln A$ ) of three stages  
84 (induction, transition and crystallization) were determined based on Arrhenius equation.

$$85 \quad \ln(1/t_0) = \ln A_0 - E_0/RT \quad (5)$$

$$\ln v_{tr} = \ln A_{tr} - E_{tr}/RT \quad (6)$$

$$\ln v_c = \ln A_c - E_c/RT \quad (7)$$

### 88 **Catalytic study:**

89 The methanol-to-hydrocarbons (MTH) reaction was performed in a fixed-bed reactor  
90 at atmospheric pressure. Typically, 0.4 g of the zeolite sample (sieve fraction, 0.25~0.5  
91 mm) was placed in a quartz reactor (5 mm i.d.) and treated with flowing helium at 450 °C  
92 for 1 h. After cooling to the desired reaction temperature of 425 °C, methanol was  
93 injected with a flow of 1 mL/h, corresponding to a weight hourly space velocity (WHSV)  
94 of 2.0 h<sup>-1</sup>. The products were analyzed by an on-line gas chromatograph Shimadzu GC-  
95 2010 Plus with flame ionization detector (FID) and a Poraplot Q-HT column (40 m ×  
96 0.18 mm × 0.18 μm). The temperature of the column was kept at 40 °C for 7 min and  
97 then increased to 200 °C at a heating rate of 10 °C/min, and then maintained at 200 °C  
98 for 4 min.

99

100

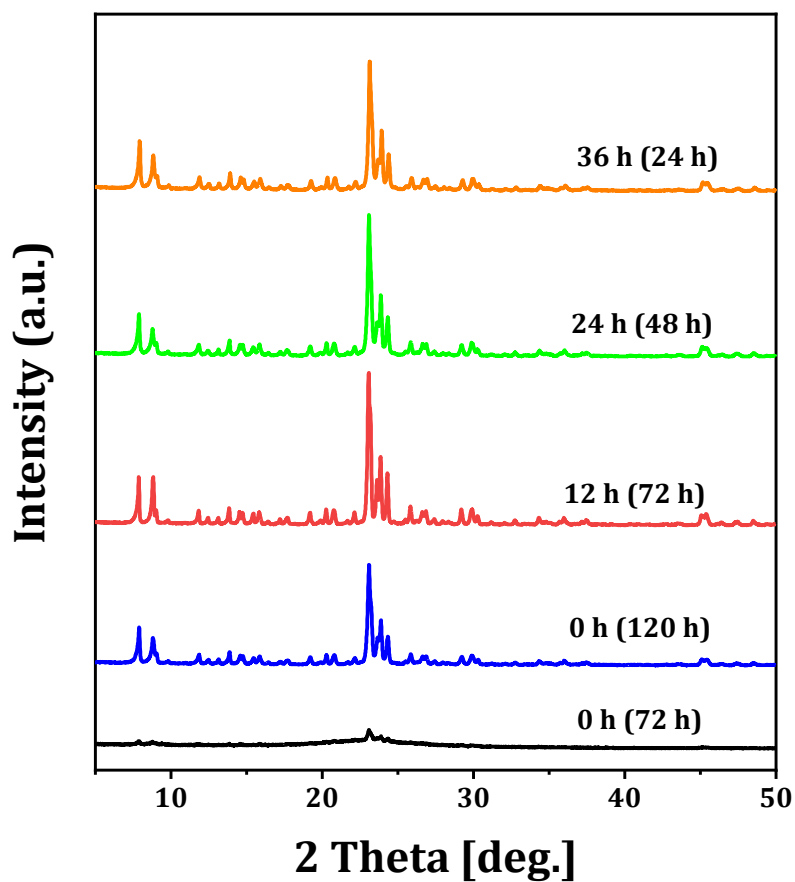
101 **Supplementary Table 1. Textual parameters from Ar adsorption-desorption tests**  
102 **of samples at different synthesis stages**

103

Sample	$S_{\text{BET}}^{\text{a}}$ ( $\text{m}^2/\text{g}$ )	$S_{\text{extra}}^{\text{b}}$ ( $\text{m}^2/\text{g}$ )	$V_{\text{Total}}$ ( $\text{cm}^3/\text{g}$ )	$V_{\text{micro}}^{\text{b}}$ ( $\text{cm}^3/\text{g}$ )
As-synthesized representing S-1 ZMN	426	71	0.23	0.14
Solid product after aging for 12 h	541	74	0.27	0.19
Solid product after pH regulation and aging for another 12 h	274	274	0.49	0

104 <sup>a</sup>: determined by the multi-point BET method105 <sup>b</sup>: calculated using the t-plot method.

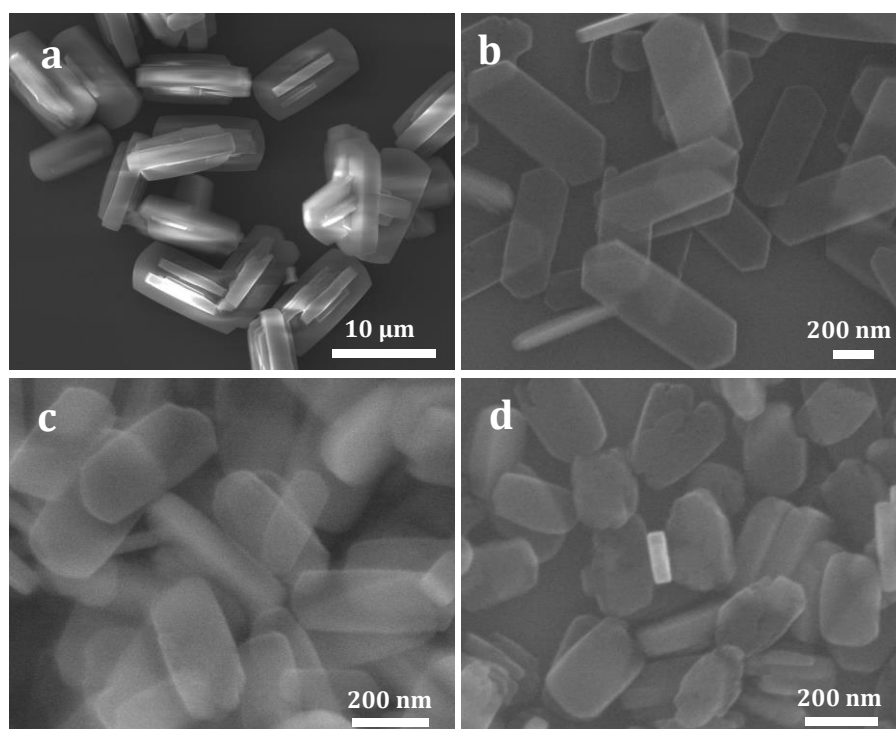
106



107

108 **Supplementary Figure 1.** XRD patterns of samples synthesized at aging temperature of  
109 90°C for different time and different crystallization time (crystallization time is shown in  
110 parentheses, crystallization temperature=120 °C)

111

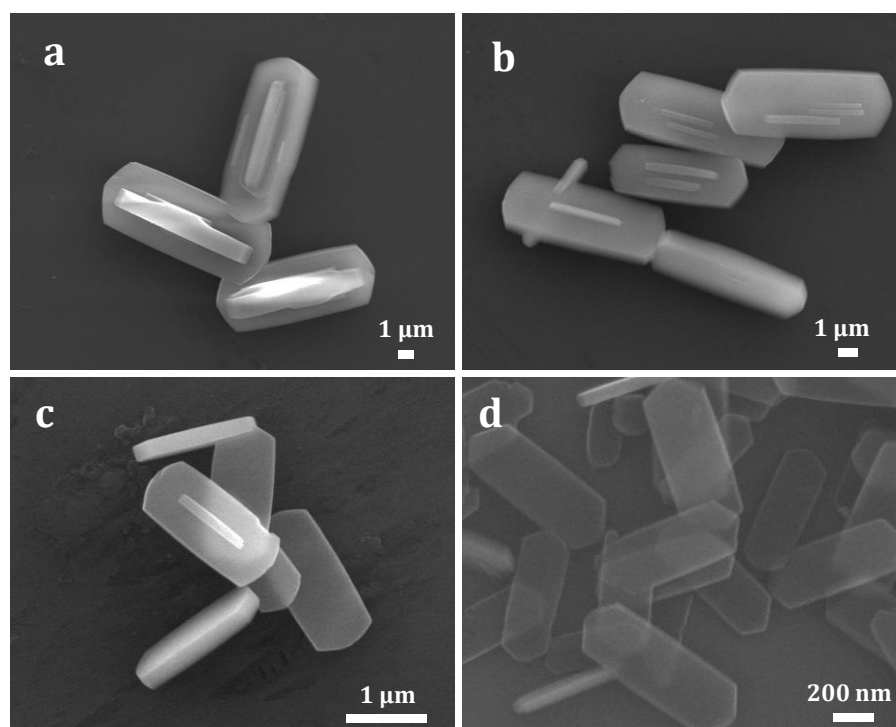


112

113 **Supplementary Figure 2.** SEM images of samples synthesized at aging temperature of

114 90°C for different time and different crystallization time: (a) 0 h, 120h; (b) 12 h, 72 h; (c)

115 24 h, 48 h; (d) 36 h, 24 h (crystallization temperature=120 °C).

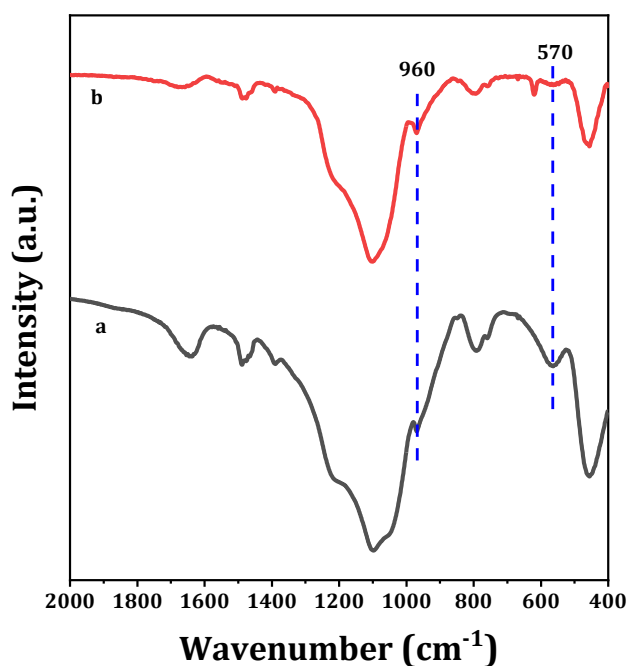


116

117 **Supplementary Figure 3.** SEM images of samples synthesized at different aging

118 temperatures for 12 h and different crystallization time: (a) 30 °C, 120 h; (b) 50 °C, 72h;

119 (c) 70 °C, 72 h; (d) 90 °C, 72 h (crystallization temperature=120 °C).

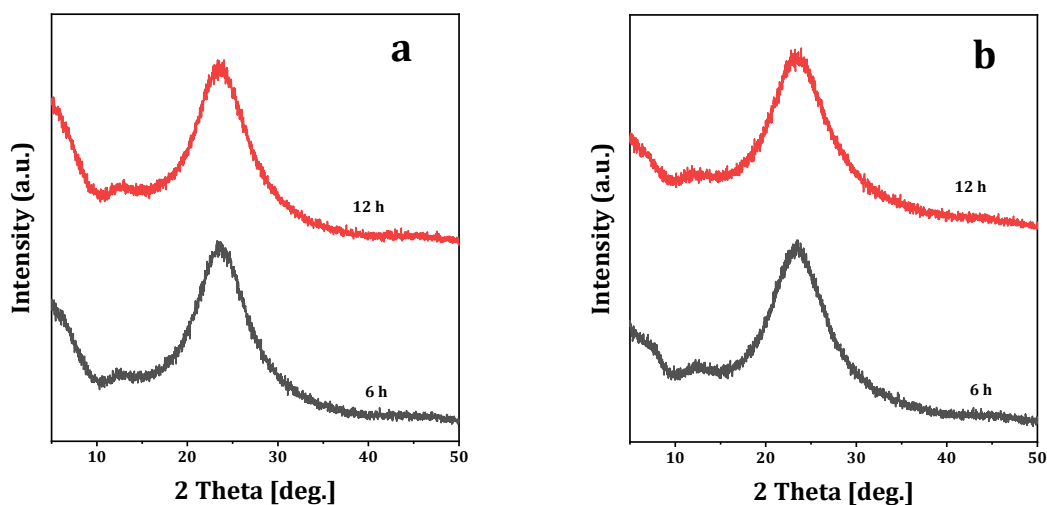


120

121 **Supplementary Figure 4.** The FTIR spectra of (a) the solid phase from the vacuum  
122 freeze-drying gel aging at 90°C for 12h and (b) the solid phase from the vacuum freeze-  
123 drying gel after regulating the pH to 8.5 and aging at 90°C for another 12h.

124

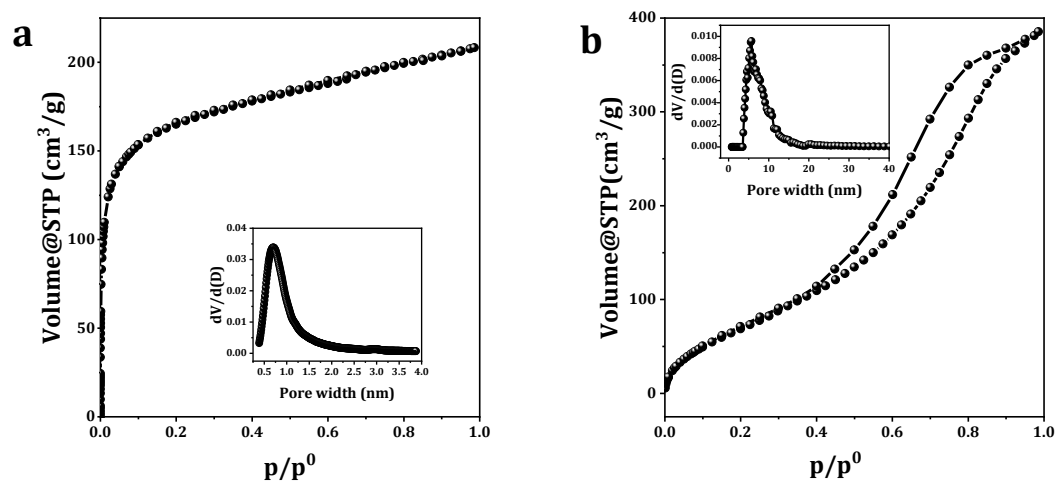
125



126

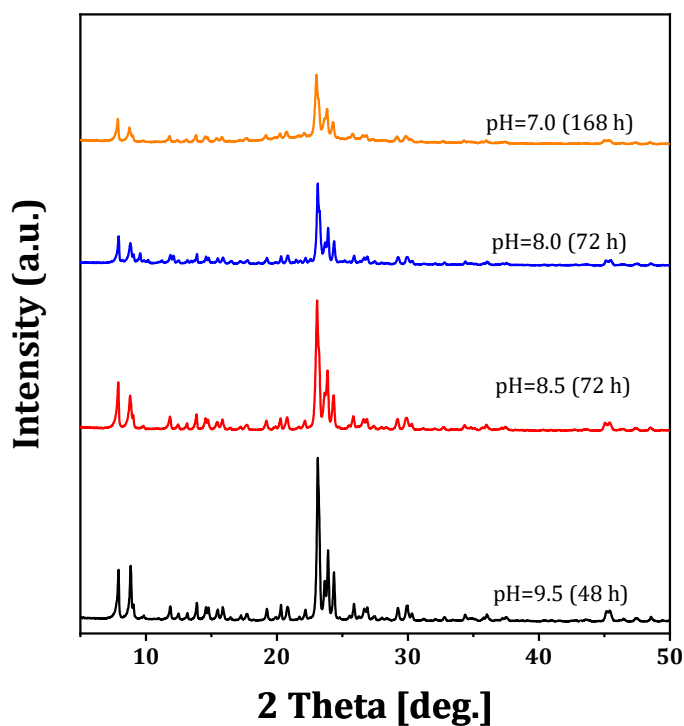
127 **Supplementary Figure 5.** XRD patterns of samples (a) after aging for 6 and 12 h, and  
128 (b) after regulating pH to 8.5 and aging for another 6h and 12h.





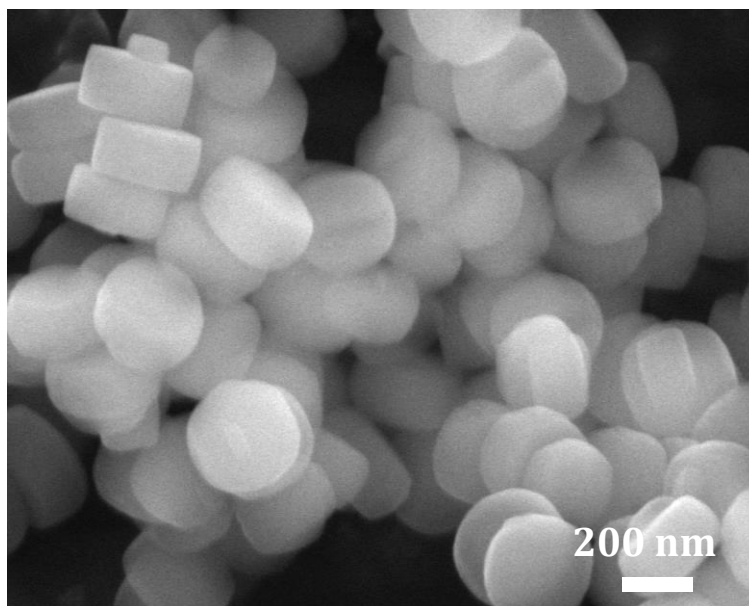
129

130 **Supplementary Figure 6.** Ar adsorption-desorption isotherms with pore size  
 131 distribution shown as insets of (a) the solid phase from the vacuum freeze-drying gel  
 132 aging at 90 °C for 12h and (b) the solid phase from the vacuum freeze-drying gel after  
 133 regulating the pH to 8.5 and aging at 90 °C for another 12h.



134

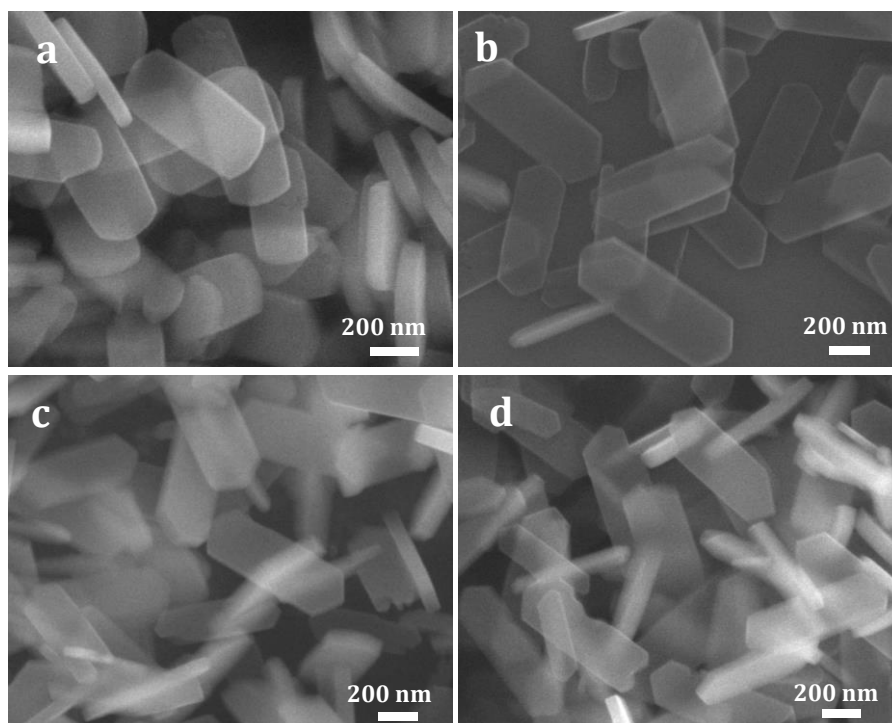
135 **Supplementary Figure 7.** XRD patterns of S-1 ZMNs synthesized at different pH of the  
 136 aging gel and different crystallization time: (a) pH=9.5, 48 h, (b) pH=8.5, 72 h, (c)  
 137 pH=8.0, 72 h, (d) pH=7.0, 168 h. Crystallization temperature: 120 °C (a, b) or 150 °C  
 138 (c, d).



139

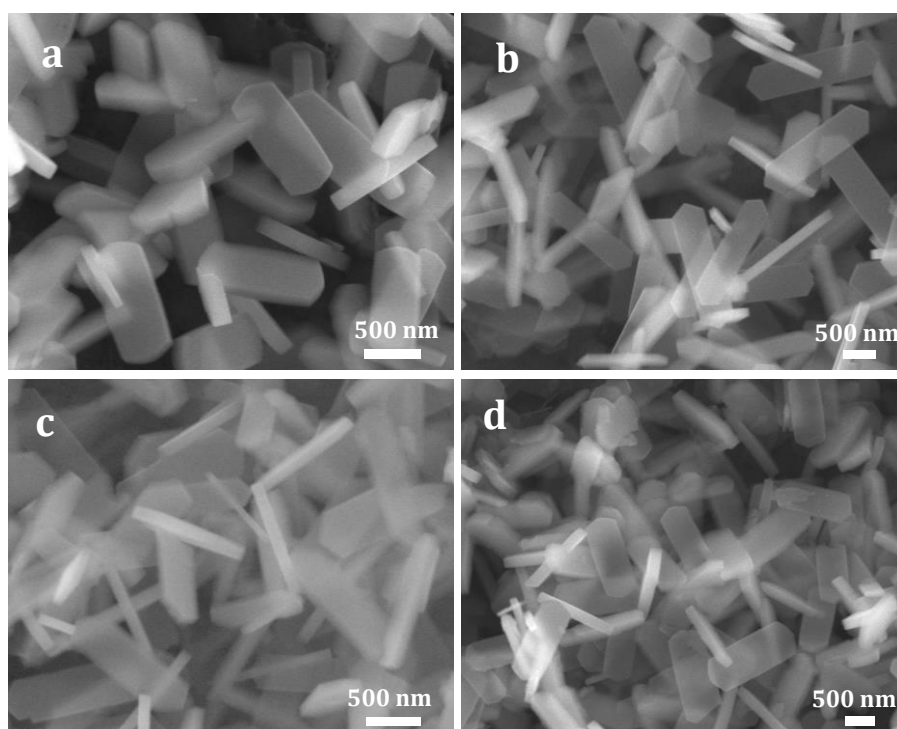
140 **Supplementary Figure 8.** SEM image of sample synthesized under the alkaline

141 condition (pH = 11.4) without pH regulation at 120 °C for 48 h.



142

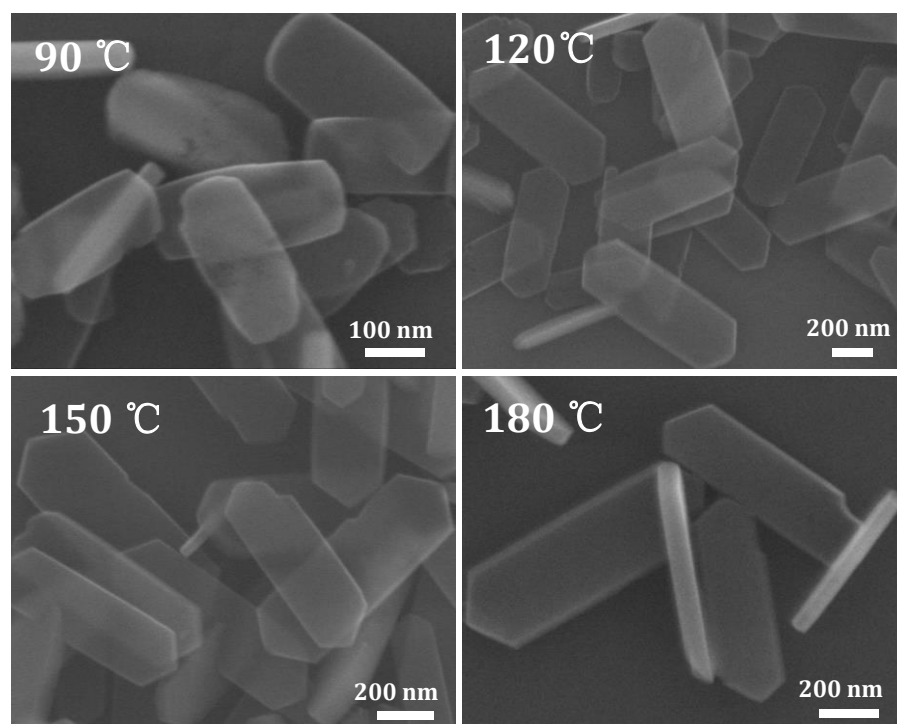
143 **Supplementary Figure 9.** SEM images of S-1 ZMNs synthesized under different  
144 anionic systems: (a) HCl, (b) H<sub>2</sub>SO<sub>4</sub>, (c) CH<sub>3</sub>COOH and (d) H<sub>2</sub>C<sub>2</sub>O<sub>4</sub>. (crystallization  
145 temperature=120 °C; crystallization time=72 h).



146

147 **Supplementary Figure 10.** SEM images of S-1 ZMNs synthesized from the system of148  $\text{SiO}_2$ : 0.15 TPAOH: 25  $\text{H}_2\text{O}$ : 0.025  $\text{MSO}_4$ , M=(a)  $\text{Li}_2$ , (b)  $\text{Na}_2$ , (c)  $\text{K}_2$  and (d) Mg.

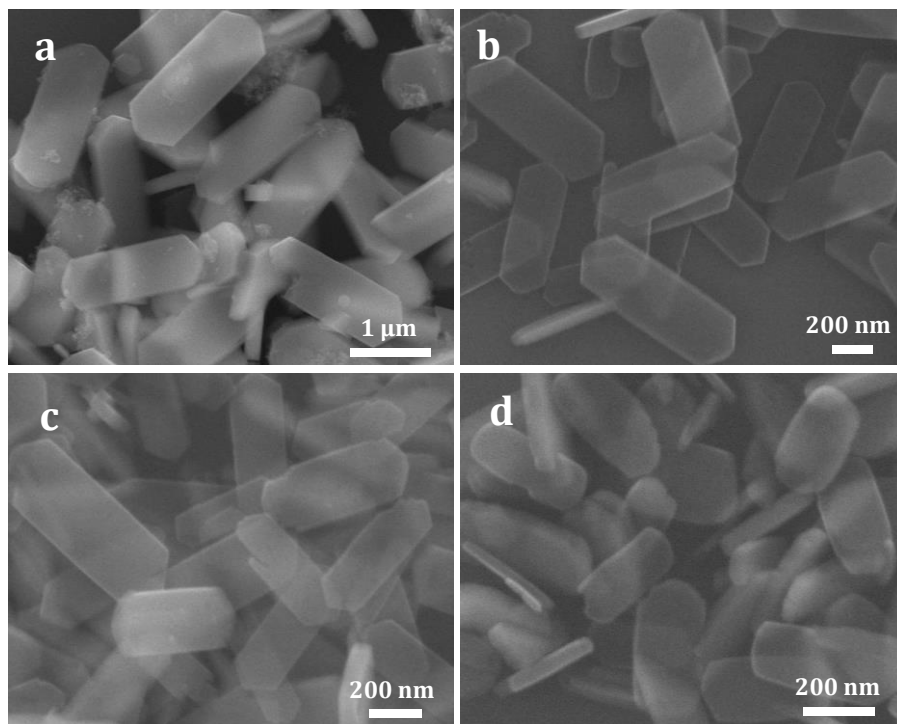
149



150

151 **Supplementary Figure 11.** SEM images of samples crystallized at 90 °C for 96 h, and

152 120, 150 and 180 °C for 72 h.



153

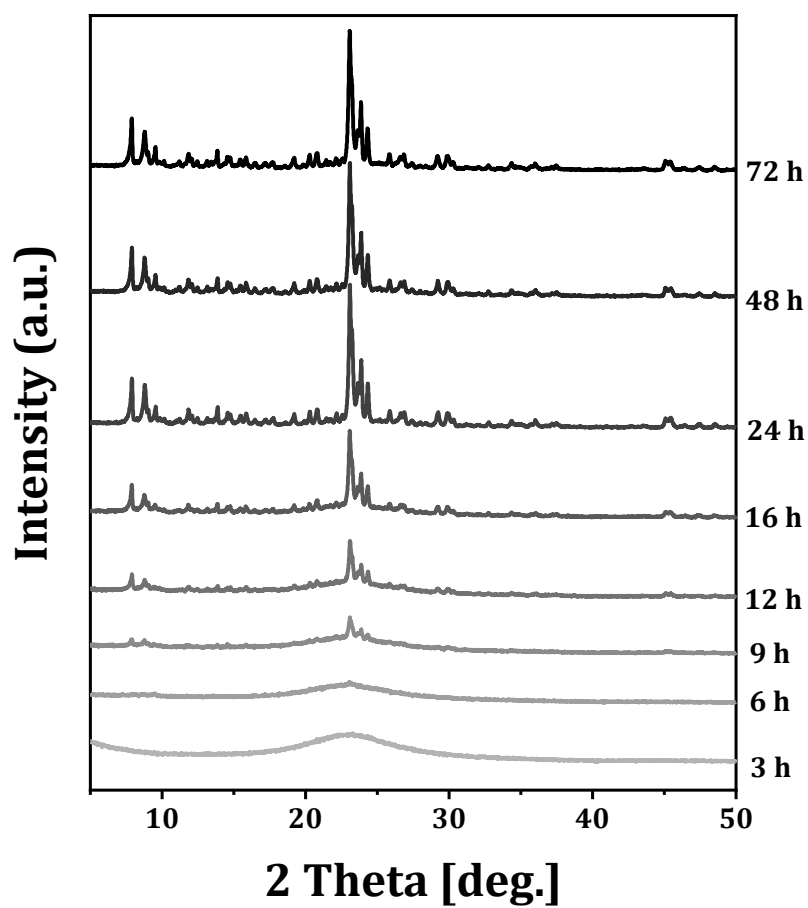
154 **Supplementary Figure 12.** SEM images of samples synthesized from the system of155 xTPAOH: 1.0 SiO<sub>2</sub>: 25 H<sub>2</sub>O, where x = (a) 0.1, (b) 0.15, (c) 0.2, and (d) 0.3

156 (crystallization temperature=120°C, crystallization time=72 h, pH=8.5).

157

158

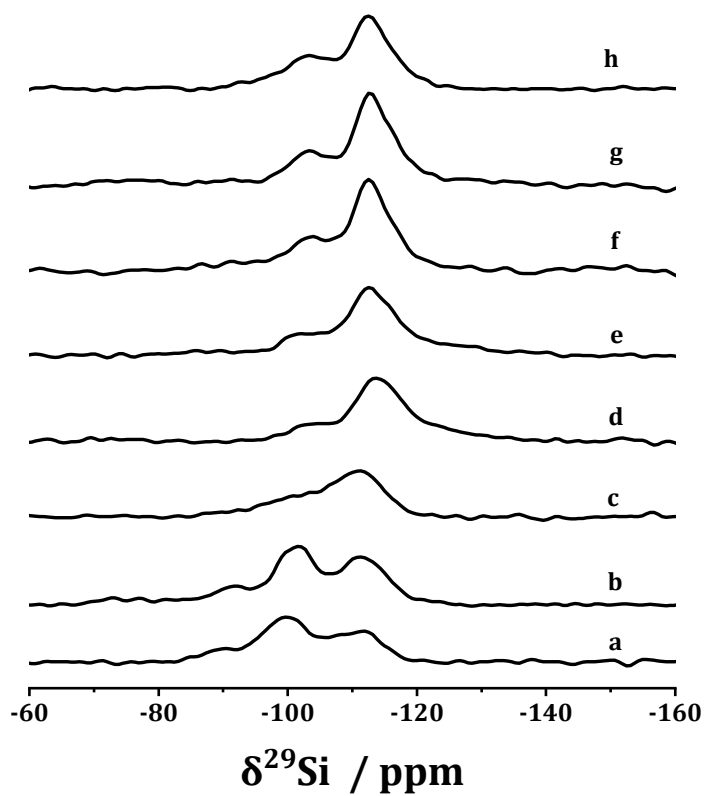
159



160

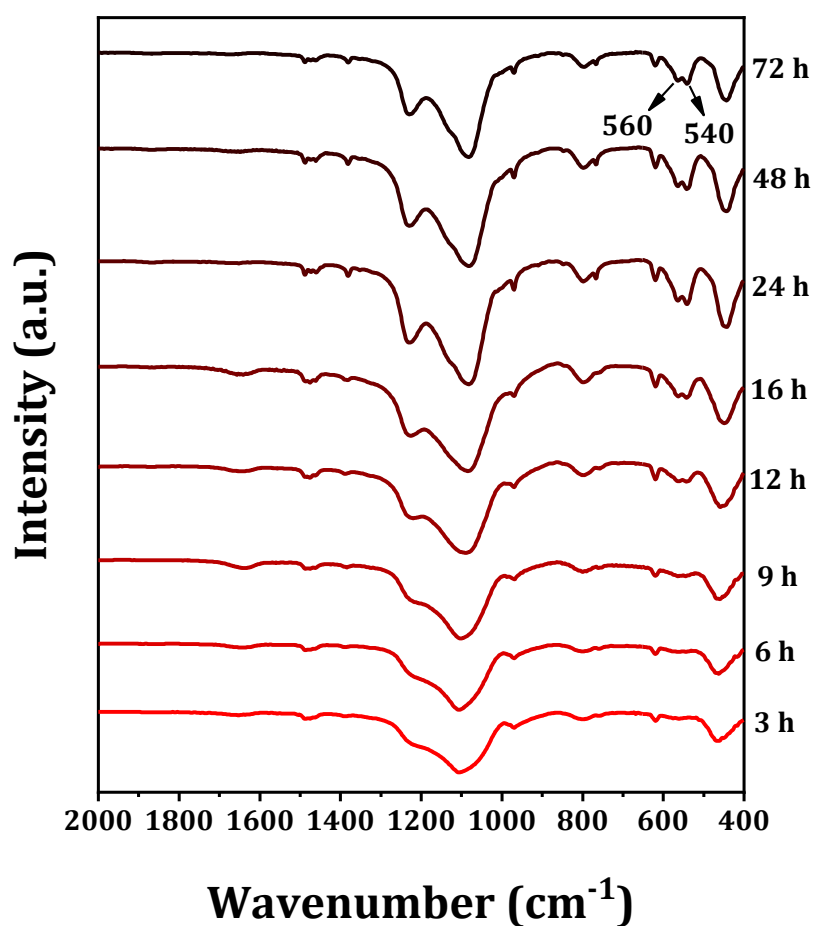
161 **Supplementary Figure 13.** XRD patterns of samples after hydrothermal treatment in the

162 autoclave for 3, 6, 9, 12, 16, 24, 48 and 72 h.



163

164 **Supplementary Figure 14.**  $^{29}\text{Si}$  MAS NMR spectra of samples at different stages of  
165 ZMN synthesis: (a) after aging at 90 °C for 12 h; (b) after regulating the pH to 8.5 and  
166 aging at 90 °C for another 12 h; after hydrothermal treatment in the autoclave for (c) 6,  
167 (d) 12, (e) 16, (f) 24, (g) 48 and (h) 72 h.



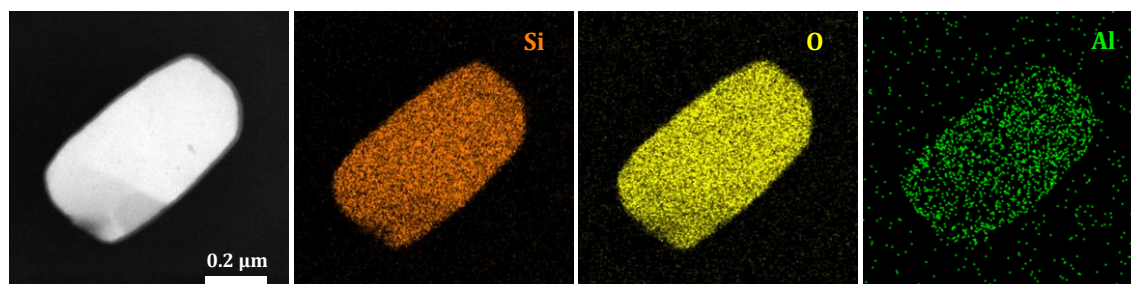
168

169 **Supplementary Figure 15.** The FT-IR spectra of samples after hydrothermal treatment  
170 in the autoclave for 3, 6, 9, 12, 16, 24, 48 and 72 h.

171

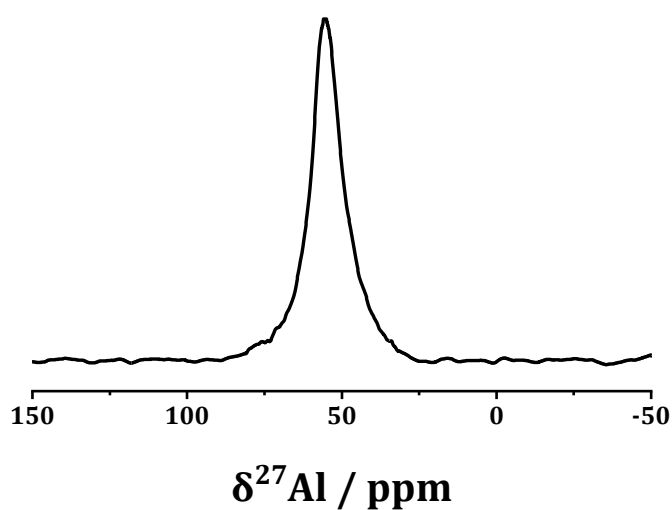
172

173



174

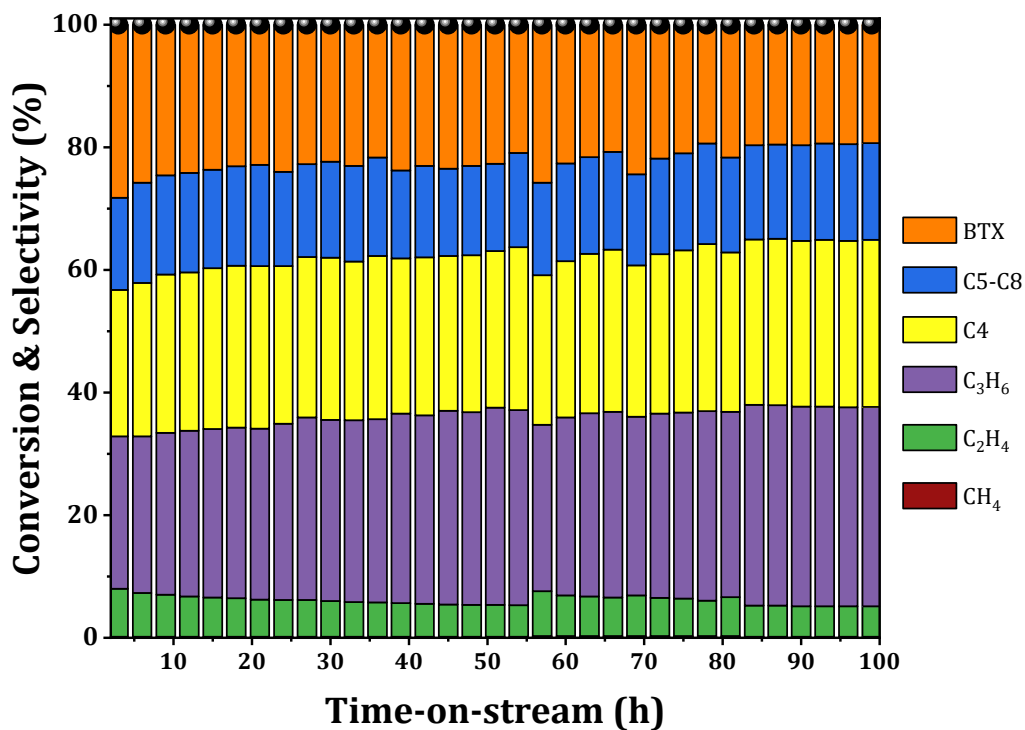
175 **Supplementary Figure 16.** TEM images of a single ZSM-5 ZMN crystal and the  
176 corresponding element mapping analysis.



177

178

**Supplementary Figure 17.**  $^{27}\text{Al}$  MAS NMR spectrum of as-synthesized ZSM-5 ZMN.



179

180

181

182

183

184

**Supplementary Figure 18.** Methanol conversion and product selectivity as a function of time over ZSM-5 ZMNs in MTH reaction. Reaction conditions: 0.4 g catalyst, WHSV = 2 h<sup>-1</sup>, T= 425 °C, ambient pressure.



185 **REFERENCES**

- 186 1. Thompson RW. Analysis of Zeolite Crystallizations Using Avrami Transformation  
187 Methods. *Zeolites* 1992; 12: 680–684. [DOI: 10.1016/0144-2449(92)90115-6]
- 188 2. Corregidor PF, Acosta DE, Destéfanis HA. Kinetic Study of Seed-Assisted  
189 Crystallization of ZSM-5 Zeolite in an OSDA-Free System Using a Natural  
190 Aluminosilicate as Starting Source. *Ind Eng Chem Res* 2018; 57: 13713–13720. [DOI:  
191 [10.1021/acs.iecr.8b03487](https://doi.org/10.1021/acs.iecr.8b03487)]
- 192 3. Kim SD, Noh SH, Seong KH, Kim WJ. Compositional and Kinetic Study on the Rapid  
193 Crystallization of ZSM-5 in the Absence of Organic Template under Stirring. *Micropor*  
194 *Mesopor Mater* 2004; 72: 185–192. [DOI: 10.1016/j.micromeso.2004.04.024]